Magnetic-Field-Guided Motion of Electrons in a Bulk Semiconductor

H. Sigg[a] and K. Ploog
Max-Planck-Institut für Festkörperforschung, 7000 Stuttgart 80, Federal Republic of Germany

Qiu-Yi Ye and F. Koch
Physik Department E16, Technische Universität München, 8046 Garching, Federal Republic of Germany
(Received 4 December 1989)

The free-electron cyclotron resonance in *n*-type GaAs with rather weak impurity doping in a regular sequence of sheets shows a strong dependence of the carrier scattering rate on the direction of the applied magnetic field **B**. For the case of **B** directed exactly along the sheets we find a linewidth narrowing of more than a factor of 4. This effect is due to the **B**-aligned trajectory of the circling electrons which extends along, but outside of, the doping sheets. Our experiment is the direct observation of an anisotropic distribution of scatterers in an otherwise isotropic semiconductor.

PACS numbers: 72.20.−i, 76.40.+b

It is well known that high-mobility carrier systems can be obtained by the controlled positioning of donors in layered semiconductor systems, as, e.g., in AlGaAs/GaAs heterostructures.[1] In such systems the reduced carrier scattering is due to the confinement of the carriers at the heterointerface far away from their parent ionized donors. In this paper we will present another way to achieve a mobility enhancement in semiconductors. We consider the magnetic guiding of electrons in *n*-type GaAs having a spatially isotropic band structure (no confinement) but an anisotropic distribution of scatterers. Our experiments resemble earlier work on magnetic size effects in systems with scattering length larger than the sample dimensions; examples for such work are magnetotransport studies in small metallic samples[2] and the ballistic transport in one- and two-dimensional systems.[3]

The measurements are performed on *n*-type GaAs samples with impurity doping in a regular sequence of monolayer sheets. The state-of-the-art growth technique of molecular-beam epitaxy (growth temperature $T \simeq 500\,^{\circ}\mathrm{C}$ and doping during the interruption of the growth[4]) has been applied in order to get the Si donors embedded as sheets in atomically narrow planes. Twenty consecutive doping sheets spaced 1000 Å apart are sandwiched by 0.5-μm-thick buffer and cap layers. The background doping level in these layers is estimated to be $(1-3)\times 10^{14}\ \mathrm{cm}^{-3}$ *p* type. For the sample investigated, the Si-donor sheet density, as determined by Hall measurements, is $N_D \simeq 2.2\times 10^{11}\ \mathrm{cm}^{-2}$. This doping level corresponds to a mean in-plane distance of the Si donors of 2–3 times the effective Bohr radius of $a_B^* \simeq 100$ Å. Perpendicular to the planes the donor distance, and hence the mean scatterer distance, is much larger and is given by a layer spacing of 1000 Å. Because of the small donor wave-function overlap, confinement effects as observed for the so-called δ-doped GaAs systems with V-shaped potential[5] do not occur. Instead, at helium temperature the electrons are frozen out on the individual donors and the transport is found to be in-plane hopping of electrons from donor to donor site.[6] The far-infrared (FIR) response is the resonance of hydrogenic impurity states.[7]

Here we report a study of the free cyclotron resonance (CR) that can be observed for thermally activated electrons at temperatures $T \geq 10$ K. The FIR transmission and photoconductivity measurements have been performed with the sample mounted in a top-loading variable-temperature cryostat. The magnetic fields are generated by a superconducting solenoid. The measurements are performed at constant laser radiation wavelength λ while sweeping the magnetic field through the resonance. A light-pipe system consisting of brass tubes, flat mirrors, and Winston cone is used to focus FIR radiation on the sample. Indium dots annealed for 5 min at

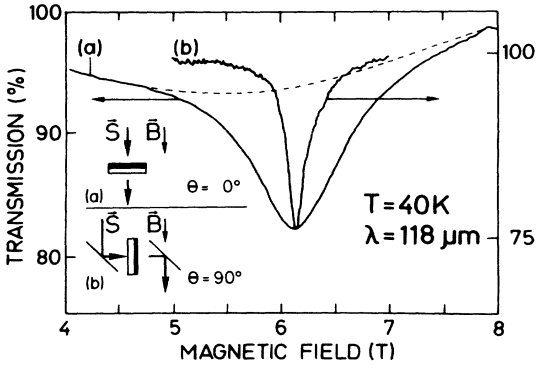

FIG. 1. CR measured in transmission at temperature $T=40$ K and wavelength $\lambda=118$ μm. Curve *a* is obtained in the Faraday configuration where the magnetic field is parallel to the sample normal, and curve *b*, the Voigt configuration with sample tilted at $\Theta=90°$ (see inset). The dashed line gives the residual transmission signal due to the impurity-bound resonance.

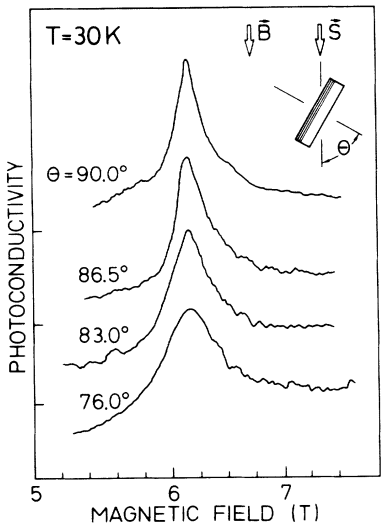

FIG. 2. Photoconductivity response of the CR for sample orientations close to and exactly at $\Theta=90°$. For the definition of the angle Θ, see inset.

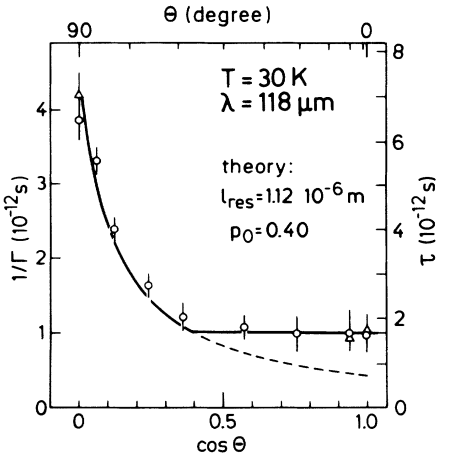

FIG. 3. Angular dependence of $1/\Gamma$, the inverse of the experimentally determined half width at half maximum. The dots and triangles are obtained from a linewidth analysis of, respectively, the photoconductivity (○) and transmission (△) measurements. The solid lines give the calculated scattering time τ using the indicated values for the probability p_0 for an electron to get scattered on crossing a doping sheet, and residual scattering length l_{res}. Note that the comparison between the left- and right-hand scales of the y axes yields $\Gamma\tau\simeq 1.7$.

400 °C provide the Ohmic contacts for the photoconductivity measurements.

The CR has been investigated for three different configurations: In transmission (at normal incidence of the radiation), with the sample normal parallel (Fig. 1, curve *a*) and perpendicular (Fig. 1, curve *b*) to the magnetic-field axes and, in photoconductivity, at various angles Θ from 0° to 90° (Fig. 2). The data of Fig. 1 show a remarkable narrowing of the CR linewidth, observed simply by tilting the sample from $\Theta=0°$ to $\Theta=90°$. The temperature and laser wavelength were in both configurations $T=40$ K and $\lambda=118$ μm, respectively. The narrow CR line for $\Theta=90°$ (sample normal perpendicular to the magnetic field) is also evident from the photoconductivity measurements shown in Fig. 2. In order to increase the signal, these measurements are taken at $T=30$ K with the laser wavelength being again $\lambda=118$ μm. We emphasize that—in contrast to the linewidth—the resonance position does not depend on the angle Θ. This indicates that confinement effects which would lead to a $1/\cos\Theta$ or similar behavior do indeed not appear. The electronic band structure of the sample is bulklike and thus isotropic.[8]

From Fig. 1 one finds that the integrated absorption for the two CR measurements differs by about a factor of 2. This is expected because of the different configurations used. Figure 1, curve *a* refers to the Faraday configuration which has a CR oscillator strength for unpolarized light that is twice as strong as that for the Voigt configuration (Fig. 1, curve *b*). It was difficult to obtain a more quantitative comparison of the transmission strength because of the background signal of the impurity-related resonance (dashed line in Fig. 1) and the signal saturation of the narrow resonance at almost 75%, the minimum transmission for the Voigt configuration. Still, the applied line-fitting procedure gives evidence for a somewhat smaller integrated CR transmission strength at $\Theta=90°$.

The configurations for the photoconductivity measurements are not well defined. At $\Theta=90°$, the laser light enters the sample from the edge—this is the Faraday configuration. Furthermore, stray light may enter the sample from its face, with propagation almost perpendicular to the direction of the magnetic field. However, the fact that exactly the same narrow CR line is observed in both the true Voigt configuration of Fig. 1, curve *b*, and in the mixed configuration of Fig. 2 ($\Theta=90°$) means, in our view, that the direction of light propagation is not essential for the observed CR linewidth. Obviously, collective effects like a plasmon shift are not expected because of the rather low doping concentration. In fact, we will show that it is simply the direction of the magnetic field with respect to the sample that determines the CR linewidth. From symmetry arguments we deduce that this effect must be related to the only anisotropy in the system, i.e., the doping sheets.

The results of Fig. 2 demonstrate that already a small deviation from the perpendicular configuration with $\Theta=90°$ leads to a substantial increase of the linewidth. The full angular dependence of the CR linewidths, obtained in the photoconductivity configuration (Fig. 2), is shown in Fig. 3. For convenience, we plot the inverse of the half-width Γ in the frequency domain. Γ is converted from ΔB, the measured full width at half maximum, making use of the almost linear dependence of the CR transition energy on the magnetic field, $\omega_c=(e/m^*)B$.

Thus, the linewidth Γ is given by $(e/m^*)\Delta B/2$, where m^* is the measured effective mass $m^* \simeq 0.07 m_e$. The most striking features of Fig. 3 are the steep decrease of $1/\Gamma$ in the interval $90° > \Theta \geq 65°$ and the almost perfect independence of Γ on Θ for $\Theta \leq 65°$. In the following we will discuss this angular dependence of the linewidth in terms of a scattering rate τ.

Our simple classical model is based on a straightforward consideration of the magnetic-field-induced-guided motion. Figure 4 illustrates the well-known spiraling motion of electrons on cylinders having axes parallel to the direction of the applied magnetic field. The radius of the cylinders depends on the magnetic field and velocity of the carriers v and is given by the classical cyclotron orbit $l_c = v/\omega_c$.[9] As we are in the nondegenerate limit, the velocity v is given by Boltzmann statistics; i.e., in the average we have $m^* \bar{v}_{\rm th}^2/2 \simeq kT$. At $B = 6$ T and $T = 40$ K, l_c is about 85 Å and therefore much smaller than the interlayer distance of $a = 1000$ Å. From Fig. 4 it becomes evident why our CR experiment, at, respectively, $\Theta = 0°$ and $\Theta = 90°$ resolves the apparent anisotropy in the scatterer distribution. At angle zero, the scattering length is determined by the probability, p_0, for electrons to be scattered on their way through a doping sheet. However, for B parallel to the layers ($\Theta = 90°$), the helixes do not cross any doping sheet. The electrons are traveling either within or outside of the doping sheets. Obviously, the in-plane carriers are immediately scattered and will therefore not appear in the CR spectra. In contrast, the electrons remaining outside of the sheets —similar to the case of remote doping in heterostructures—exhibit a rather high mobility and therefore lead to the narrow CR signal. The mentioned lack of integrated transmission strength at $\Theta = 90°$ is, perhaps, due to the missing strongly scattered in-plane carriers. Further support for our simple model is found from the description of the angular dependence of the CR

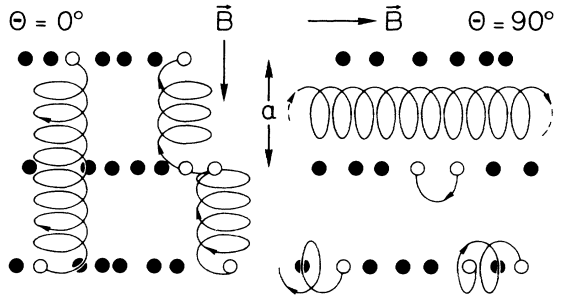

FIG. 4. Schematic illustration of the helical motion of electrons along the direction of the magnetic field **B**. For the case of **B** perpendicular to the doping sheets, the carriers are forced to cross the doping sheets and are therefore effectively scattered. For the case where **B** is exactly parallel to the sheets, the carriers in between the sheets do not cross them and they move over much longer distances.

linewidth. From the well-known relation that $1/\Gamma$ is proportional to the scattering time we obtain from Fig. 3, $\tau(\Theta = 90°) \simeq 4.5\tau(\Theta = 0°)$. At $\Theta = 90°$ the scattering is that much reduced because it is expected to occur only by residual impurity atoms and by the long-range potential fluctuations originating from the in-plane ionized donors. For the following discussion, the length that defines the strength of these residual scattering processes will be denoted as $l_{\rm res}$ and will be used—together with p_0—as a parameter to calculate the full angular dependence.

At small angles, the scattering time will be given by $t_0/(p_\Theta \cos\Theta)$, where p_Θ is the angular-dependent "sticking" probability and $t_0 = a/\bar{v}_{\rm th}$ is the average time of flight for electrons at $\Theta = 0°$ to travel from one doping sheet to the next. Using a simple scattering cross-section argument, we expect p_Θ to be proportional to the number of scatterers within the area defined by the intersection of a doping sheet with a cylinder of diameter $2l_c$. Therefore, p_Θ is given by $p_0/\cos\Theta$ and, as in the case of bulk doping, the scattering time does not depend on Θ, i.e., $\tau_\Theta = t_0/p_0$. This simple consideration, however, must break down when $p_0/\cos\Theta$ is approaching unity, i.e., when the probability for an electron to cross a doping sheet without being scattered becomes zero. Then, and for $\cos\Theta < p_0$, the mean scattering time should be just the time of flight for a single crossing, i.e., $\tau_\Theta = t_0/\cos\Theta$. In order to account for the residual-impurity-induced lower limit of the scattering time $\tau_{\rm res} = l_{\rm res}/\bar{v}_{\rm th}$, we expect that for independent scattering processes the total scattering rate is given by $\tau_{\rm tot}^{-1} = \tau_{\rm res}^{-1} + \tau_\theta^{-1}$.

The data of Fig. 3 show that the angular-dependent scattering rate $\tau_{\rm tot}$ describes the experimental data extremely well. This result clearly demonstrates the validity of our concept of magnetic-field-induced-guided motion of free carriers. In particular, we can now explain the sudden increase in the scattering time at an angle of about 65° from the fact that p_0 is about 0.4; i.e., for $\Theta = 0°$, the average number of doping sheets that are passed by the carriers before being scattered is 2.5. The observation of a 4.5-times-reduced linewidth at $\Theta = 90°$ means that the scattering length $l_{\rm res}$ is a factor of 4.5 longer than $l(\Theta = 0)$; thus $l_{\rm res} \simeq 1.1$ μm.

Considering basic principles, the microscopic scattering time is related to the linewidth by $\Gamma\tau \simeq 1$. For a classical oscillator with velocity damping one obtains that $\Gamma\tau$ is exactly 1 and the relaxation is exponential in time. An experimental determination of Γ and τ, however, is very difficult and usually not very clear. The CR linewidth in two-dimensional electron systems, e.g., is sometimes orders of magnitude smaller than the scattering rate obtained from the dc mobility.[10] Here, we obtain the scattering time from the microscopic parameters p_0 and $l_{\rm res}$ applying a simple qualitative analysis of the angular-dependent CR experiment. Therefore, our experiment and the model with known values for $\bar{v}_{\rm th}$ and a

enable the independent determination of both the linewidth and the scattering time. This important result is indicated in Fig. 3 where the y axes on the left and on the right give, respectively, $1/\Gamma$ and τ_{tot}. From the perfect agreement of theory and experiment we thus conclude that for thermally activated electrons scattered on donor impurities, $\Gamma\tau \simeq 1.7$. This value, slightly larger than 1, perhaps reflects the fact that the scattering occurs at the individual doping sheets, and, therefore, the momentum relaxation is nonexponential. However, for a more rigorous discussion of the involved scattering process we would have to improve our model. So far, in this simple (and strictly classical) model, we have neglected any possible energy dependence of the scattering rate and nonparabolicity-induced inhomogeneous broadening, and we have not considered the finite extension of both donor and electron wave functions. Future experiments are planned to investigate these questions in more detail.

In summary, we have investigated the anisotropic scatterer distribution in n-type GaAs with a layered sequence of impurity sheets by measuring the configuration dependence of the free-electron cyclotron resonance. We applied the simple and classical model of guided motion along the magnetic-field lines and obtained an excellent description for the angular-dependent CR data. This new kind of CR experiment gives a way to investigate many presently unknown microscopic details of the scattering of thermally excited electrons on neutral and ionized impurities.

We acknowledge financial support from the Bundesministerium für Forschung und Technologie (BMFT) of the Federal Republic of Germany.

[a]Present address: Paul Scherrer Institute–Zürich, Badenerstrasse 569, CH-8048 Zürich, Switzerland.

[1]R. Dingle, H. L. Störmer, A. C. Gossard, and W. Wiegmann, Appl. Phys. Lett. **33**, 665 (1978).

[2]For a recent review, see A. B. Pippard, in *Magnetoresistance in Metals,* edited by A. M. Goldman, P. V. E. McClintock, and M. Springford, Cambridge Studies in Low Temperature Physics (Cambridge Univ. Press, Cambridge, 1989).

[3]H. van Houten, C. W. J. Beenakker, J. G. Williamson, M. E. I. Broekaart, P. H. M. van Loosdrecht, B. J. van Wees, J. E. Mooji, C. T. Foxon, and J. J. Harris, Phys. Rev. B **39**, 8556 (1989).

[4]K. Ploog, J. Cryst. Growth **81**, 304 (1987).

[5]A. Zrenner, H. Reisinger, F. Koch, and K. Ploog, in *Proceedings of the Seventeenth International Conference on Physics of Semiconductors, San Francisco, 1984,* edited by J. D. Chadi and W. A. Harrison (Springer-Verlag, Berlin, 1985), p. 325.

[6]Qiu-Yi Ye, A. Zrenner, F. Koch, and K. Ploog, Semicond. Sci. Technol. **4**, 500 (1989).

[7]Qiu-Yi Ye, A. Zrenner, F. Koch, H. Sigg, D. Heitmann, and K. Ploog, in Proceedings of the Fourth International Conference on Modulated Semiconductor Structures, Ann Arbor, Michigan, 1989 [Surf. Sci. (to be published)].

[8]The anisotropy in the CR of n-type GaAs at 6 T is less than 10^{-2} T and therefore is neglected; H. Sigg, J. A. A. J. Perenboom, P. Pfeffer, and W. Zawadzki, Solid State Commun. **61**, 685 (1987).

[9]For internal consistency, the classical radius l_c and not the quantized cyclotron orbit $l=(\hbar/eB)^{1/2}$ has been used. However, the consideration of l instead of l_c would not effect any of the given results.

[10]J. Richter, H. Sigg, K. von Klitzing, and K. Ploog, Phys. Rev. B **39**, 6268 (1989).